RSC Advances




ROYAL SOCIETY OF CHEMISTRY

www.rsc.org/advances

RSC Advances

PAPER

# Hydrophilic Sulfonic Acid- Functionalized Micro-Bead Silica for Dehydration of Sorbitol to Isosorbide

Received 00th January 20xx,
Accepted 00th January 20xx

DOI: 10.1039/x0xx00000x

www.rsc.org/advances

Jun Shi, Yuhua Shan*, Yuan Tian, Yu Wan, Yitian Zheng and Yangyang Feng

Different (3-Mercaptopropyl) trimethoxysilane (MPTS) loadings of sulfonic acid-functionalized micro-bead silica (SA-$SiO_2$) were prepared by silylation and oxidation, and characterized by Elemental analysis, SEM, FT-IR, TGA, $NH_3$-TPD, BET $N_2$ adsorption-desorption and $^{13}C$ NMR CP/MAS. The as-prepared SA-$SiO_2$ showed high hydrophilic nature and excellent catalytic perfomance for dehydration of sorbitol to isosorbide. The selectivity to isosorbide is obviously affected by the MPTS loading. Using SA-$SiO_2$ as a solid catalyst with 60.5% MPTS loading, 100% sorbitol conversion and 84% yield of isosorbide are achieved at 120 ℃ for 10 h under vacuum. The catalyst was reused for 10 times without noticeable loss of activity and selectivity.

## Introduction

With environmental concerns, use of green and renewable raw materials to produce chemicals has become the trend of the times. Therefore, the interest in biomass conversion into chemicals increased rapidly during the last few years.[1-6] Today, sorbitol, can be conveniently obtained from cellulose (considered the most abundant and cheap carbon source)[7-9] via glucose, is one of the "top ten" platform chemicals in biorefinery by US Department of Energy,[10-14] and its most popular dehydrated production is isosorbide[15] – an important platform chemical for the replacement of traditional oil resource products in the future.[16-20]

The dehydration of sorbitol to isosorbide (Scheme 1) is conventionally using liquid acid like sulphuric acid, hydrochloric acid and p-toluenesulfonic acid as a homogeneous catalyst in industrial production, which provides a yield of isosorbide (70-77%) at 130 ℃ under high vacuum conditions within a few hours.[21] But use of homogeneous catalysts introduces many troubles such as difficulties in product separation, a corrosive hazardous for the reactors and catalyst regeneration from the reaction system.[20] Without adding any acid catalyst, dehydration of sorbitol in high temperature water (250-300 ℃) for 1 h, 57% yield of isosorbide was obtained, reported by Yamaguchi et al.[20, 22] In addition, dehydration of pure sorbitol under microwave at 160 ℃ showed sorbitol conversion and isosorbide selectivity of 100% and 60%,[23] respectively.

Therefore, the research of sorbitol dehydration has been focused on developing solid acid catalysts.[17, 24-27] Many solid catalysts have been reported with different yields of isosorbide at suitable temperatures, such as sulfated copper oxides (67.3%, 200 ℃),[17] sulphated zirconia (61%, 210 ℃),[24] sulfated tin oxide (65%, 180 ℃),[25] metal phosphate (70.3%, 250 ℃),[28] molten salt hydrate medium (85%, 200 ℃),[27, 29, 30] and Amberlyst-15 resin (71.8%, 250 ℃).[31]

However, most of these catalysts require comparatively high reaction temperature (200-300 ℃) and yield of isosorbide is not high. Therefore, the development of efficient solid acid catalyst which catalyzed this reaction at moderate reaction conditions and obtained high yield of isosorbide is highly desirable.

Polymer-supported Brønsted acid catalysts: $SO_3H$–PS–$SO_3H$[32] have been used for dehydration of sorbitol at 150 ℃, with a maximum yield of 1,4-anhydro-D-sorbitol of 90% within 4 h. However, the yield of isosorbide is not high. Alternatively, a super hydrophobic mesoporous acid catalyst named as P-$SO_3H$ has been synthesized and used for dehydration of sorbitol to isosoride,[33] with a maximum yield (87%) of isosorbide at 140 ℃ within 10 h. Although these hydrophobic polymer-supported sulfonic acid catalysts show high yield, they are deactivation quickly for their surface affinity to humins and cokings.

The silica sulfuric acid (SSA) catalysts have widely been studied for a great number of acid catalyzed organic reactions due to their heterogeneous nature, cheapness and availability of the reagent.[34] A simple in situ method to prepare water-stable acidic mesoporous sulfonated silica without any surfactant or template was reported by Hasan,[35] and it has good catalytic performance of hydrolysis and alkylation reaction. Micro-bead silica has the advantage of hydrophilic, high BET-surface area and special porous structure.[36, 37] And chemical bond linking method has good prospects for industrial application since it can fix the organic groups on the carrier surface firmly.[38, 39] In this work, we report a simple and low-cost synthesis of a hydrophilic sulfonic acid-functionalized micro-bead silica

*Advanced catalysis and Green Manufacturing Collaborative Innovation Center, Changzhou University, Changzhou 213164, China E-mail: yhshan@cczu.edu.cn*
Electronic Supplementary Information (ESI) available. See
DOI: 10.1039/x0xx00000x

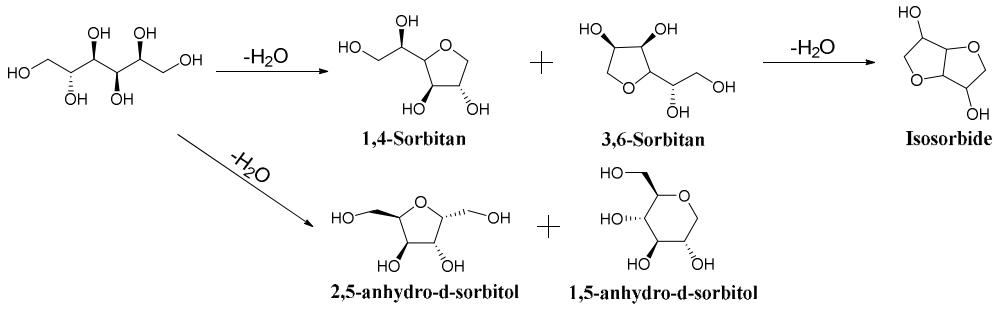


**Scheme 1** Reaction pathway of sorbitol dehydration.

catalyst named SA-$SiO_2$ and evaluated its catalytic performance in dehydration of sobitol to isosorbide in solvent free condition. As we expected, the SA-$SiO_2$ gives good sorbitol conversion and isosorbide selectivity, excellent recyclability, compared with those reported catalysts.

## Experimental Details

### Materials

Hβ (Si/Al=25), HZSM-5 (Si/Al=40), MCM-49 (Si/Al=30) were bought from Chinese NanKai University. Micro-bead silica (280~600μm) were purchased from Qingdao Haiyang Chemical Co., Ltd. (3-Mercaptopropyl) trimethoxysilane (MPTS) were purchased from Shanghai Ziyi-reagent Chemical Co., Ltd. Amberlyst-15 resin was purchased from Shanghai Host Chemical Co., Ltd. Calcium hydride ($CaH_2$), hydrogen peroxide (30% $H_2O_2$), hydrochloric acid (37% HCl), sulfuric acid (98% $H_2SO_4$), acetic acid, acetonitrile, toluene, glycol dimethyl ether, tergitol(tm)xh-(nonionic) (P123) and tetraethyl orthosilicate (TEOS) were bought from SCRC (Sinopharm Chemical Reagent Co., Ltd, Shanghai).

### Catalyst preparation

**Synthesis of SA-$SiO_2$-X.** The SA-$SiO_2$-X, sulfonic acid-functionalized micro-bead silica with different acid concentrations were prepared by loading different amount of MPTS according to the previous report,[40] and the synthetic route is shown in Scheme 2(A). The X represents the amount of MPTS loading. As a typical run, 20.0 g micro-bead silica (after washing with nitrate and roasting at 250 ℃ ) and 100 ml anhydrous toluene was charged into the flask and stirred for 30 min at room temperature. After adding 12.10 g MPTS, the mixture was refluxed under nitrogen over night.[38] Then, 20.94 g hydrogen peroxide and 3.50 g acetic acid was added dropwise and stirred for another 6 h. After washing thoroughly with acetonitrile (after drying by $CaH_2$ and redistilled) for 5 times and drying at 0.09 MPa for 5 h, the final product designated as SA-$SiO_2$-60.5 was obtained.

By adjusting the ratio of MPTS to micro-bead silica, different SA-$SiO_2$-X was obtained. For example, the catalyst loading of 60.5% MPTS was represented as SA-$SiO_2$-60.5. The elemental analysis of the SA-$SiO_2$ catalysts is shown in Table 1S.

**Synthesis of SBA-15-$SO_3H$.** The synthesis was carried out according to an established procedure,[33] and the synthetic route is shown in Scheme 2(B). As a typical run, 2.00 g P123 was dissolved in 39.75 g deionized water, and stirred for 2 h at room temperature. Then 30.0 g $H_2O$ was added and stirred for another 1 h. After adding 3.84 g TEOS, the mixture was continued to stir for 45 min. Next, 0.40 g MPTS and 4.15 g $H_2O_2$ was added sequentially and stirred for 24 h at 40 ℃. At last, the mixture was transferred into a hydrothermal reaction kettle and maintained at 100 ℃ for 24 h. The template (P123) was removed by soxhlet extraction by the mixture of

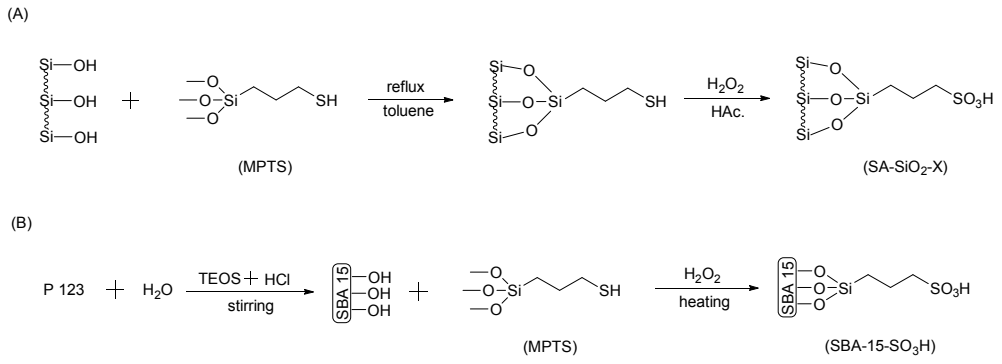


**Scheme 2** Synthetic route of SA-$SiO_2$-X and SBA-15-$SO_3H$.

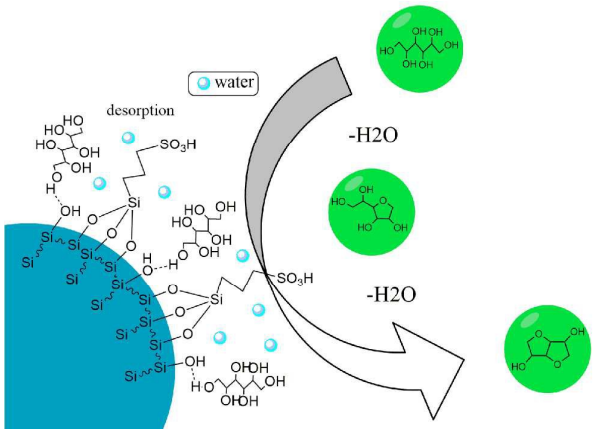


**Scheme 3** The process of sorbitol dehydration to isosorbide.

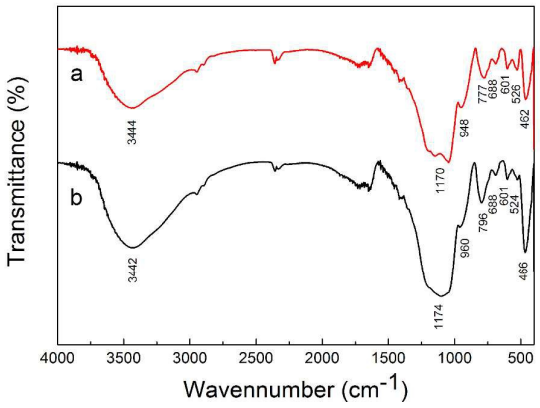


**Fig. 1** FT-IR spectra of SA-$SiO_2$ catalyst. (a) SA-$SiO_2$-60.5, (b) SA-$SiO_2$-60.5 after ten recycles.

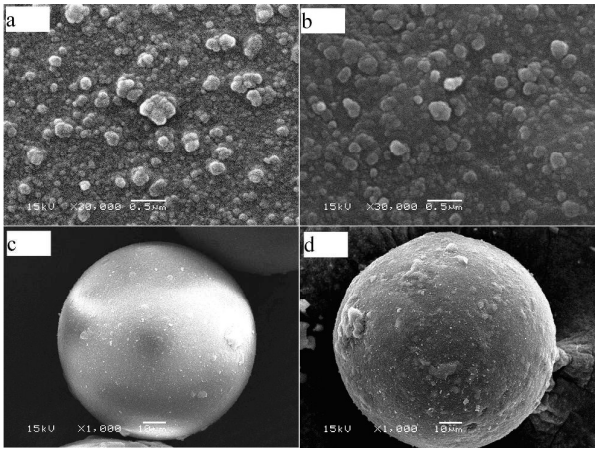


**Fig. 2** SEM images of (a) and (c) micro-bead silica, (b) and (d) SA-$SiO_2$-60.5.

hydrochloric acid and ethanol ($V_{HCl}/V_{ethanol}$=2/100). The final product designated as SBA-15-$SO_3H$ was obtained after drying at 60 ℃ for 8 h.

### Catalyst characterization

NMR spectra were collected by using a Bruker instrument (Avance Ⅲ 500MHz). The Brunauer–Emmett–Teller (BET) surface areas of catalysts were calculated according to the nitrogen adsorption–desorption isotherms method using Micromeritics ASAP2010C equipment. And before this analysis,[41] the samples were degassed at 150 ℃ for at least 10 h to remove the moisture and volatile impurities. Pore size distribution and pole volume were determined by the Density functional theory method. FT-IR spectra were carried out using a Bruker FT-IR spectrometer (TENSOR27) with a high temperature vacuum chamber.[42] Thermogravimetric analysis (TGA) measurements were carried out by a SDT Q600 instrument in the nitrogen atmosphere and the constant heating rate was 10℃ $min^{-1}$. $NH_3$-TPD was carried out in the BE-CAT-B-82 instrument equipped with a thermal conductivity detector. The scanning electron microscopy (SEM) experiments were used by scanning electron microscope (SUPRA 55 SAPPHIRE). The composition of the catalysts were analyzed by inductively coupled plasma analysis (ICP) using PerkinElmer 2400 Series Ⅱ CHNS device. The surface hydrophilicity of catalyst was measured by liquid contact angle measurement using Drop Shape Analyzer (DSA100-KRÜSS GmbH). The operation was carried out according the procedure: SA-$SiO_2$ powders were pressed into a sheet then the sheet and sorbitol/ isosorbide were putted in 100 ℃ constant temperature box for 1 h. The molten sorbitol/ isosorbide were dropped onto the SA-$SiO_2$ sheet surface rapidly and take the picture quickly. Diagram of the apparatus is shown in Fig. S6.

The acidity of the SA-$SiO_2$ catalysts was determined by acid-base titration in ultrasonic pool, according to the following definition:

$$\text{Total acidity} = (V_1 - V_0) \times C_{NaOH} / W$$

$V_0$: Standard NaOH solution volume consumed by blank sample (ml).

$V_1$: Standard NaOH solution volume consumed by test sample (ml).

$C_{NaOH}$: Concentration of standard NaOH solution (mol/L).

W: Weight of test sample (g).

### Catalyst performance evaluation and product analysis

The catalytic reaction was carried out in a 250 mL round-bottom flask equipped with a vacuum pump (in order to maintain the reaction pressure below 1000 Pa) with a magnetic stirrer (300 r.p.m.). Sorbitol (50 g) was added in a three-neck flask, followed by heating at 100 ℃ to yield clear melt. Then, the catalyst was added and the reactor was heated to reaction temperature with an oil bath pot. During the heating reaction, water was continuously removed off under reduced pressure to promote the reaction equilibrium shift to the positive direction.

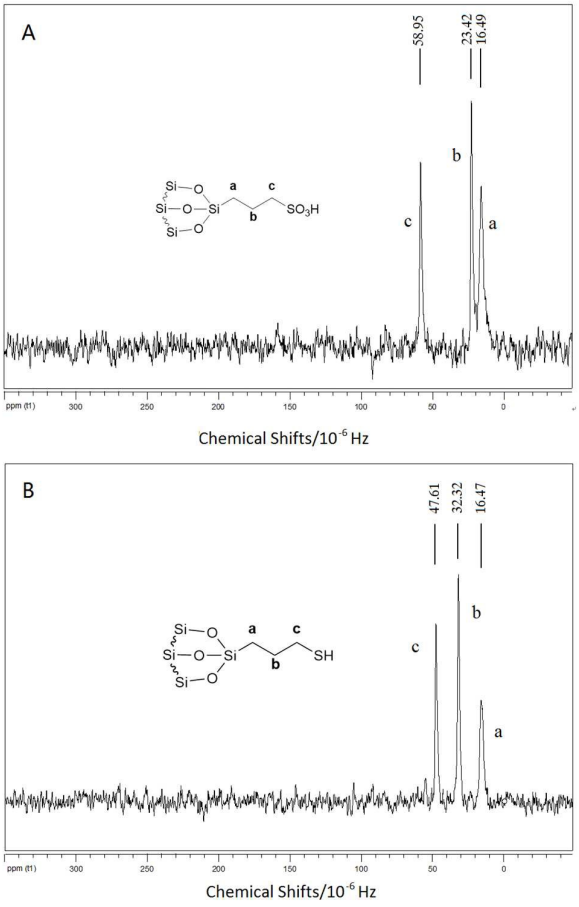


**Fig. 3** $^{13}$C NMR CP/MAS spectrum of SA-$SiO_2$-60.5 and its precursor.

Products were analyzed by HPLC (Agilent LC1260) equipped with a Zorbax $NH_2$ column (4.6*200mm, 5μm particle size) and an Evaporative Light-scattering Detector (ELSD). The sugar products were separated by reversed-phase mode. The mobile phase was acetonitrile-water (80:20) with a flow rate of 0.5 ml/min. The column was thermostated at room temperature. The selectivity or yield of sorbitan or isosorbide was based on molar composition. The isolated yield is calculated by the following definition:

$$\text{yield}_{\text{isolated}} = \text{(mol of isolated product)/(mol of sorbitol)} \times 100\%$$

**Procedure for catalyst regeneration**

To better test the stability of used catalyst, regeneration was performed with the following procedure: After reaction, the used catalyst was recycled by filtration, and washed in ultrasonic pool with water, glycol dimethyl ether, and water, sequentially to remove the coke formed in reaction, then dried at 100 ℃ for the next run.

## Results and discussion

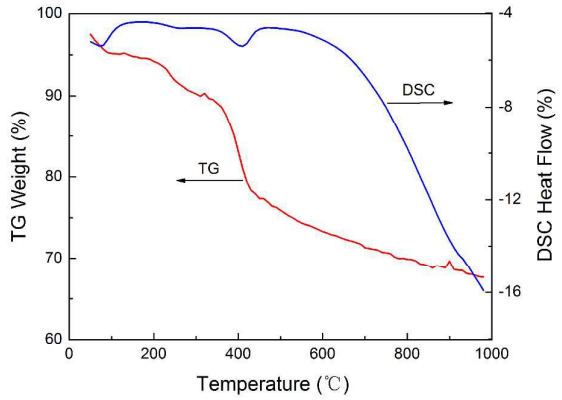


**Fig. 4** DSC-TGA curves of SA-$SiO_2$-60.5

**Catalyst characterization**

The sulfonic acid-functionalized catalyst was characterized by various physicochemical analyses. Fig.1 shows FT-IR spectra of SA-$SiO_2$-60.5 and SA-$SiO_2$-60.5 after ten recycles. The oxidation product of MPTS displays characteristic bands at 1360~960 $cm^{-1}$ and 800~510 $cm^{-1}$. The bands at 601 $cm^{-1}$ and 526 $cm^{-1}$ indicate the presence of C-S stretching vibrations bond, while the absorbance peak at about 1170 $cm^{-1}$ is associated with a sulfonic acid group because of the presence of O=S=O bond.[43] The strong and broad peak at around 3440 $cm^{-1}$ is assigned to the stretching vibration of –OH. Furthermore, the SA-$SiO_2$-60.5 catalyst shows absorbance peaks at 688, 601, and 526 $cm^{-1}$. In addition, these absorbance peaks all show red shifts due to the electron inductive effect of O=S=O double band.[44] All the results indicate successful introduction of sulfonic acid groups in the SA-$SiO_2$-60.5 sample.

The SEM images of $SiO_2$ and SA-$SiO_2$-60.5 are shown in Fig. 2. From the SEM images, it can be seen that the surface of SA-$SiO_2$-60.5 catalyst is rough while that of the micro-bead silica is relatively smooth. It is caused by the sulfonic acid groups chemically bonded on the micro-bead silica.

The (CP/MAS) $^{13}$C-NMR spectrum of SA-$SiO_2$-60.5 and its precursor (unoxidized product) is shown in Fig. 3. The chemical shifts of saturated carbon are generally at 0~70, while that of the unsaturated carbon are usually at 100~165. As shown in Fig. 3A, the chemical shift peaks at 16.49 and 23.42 are associated with the saturated carbon atom attached to a silicon atom and saturated carbon atom attached to a carbon atom of both ends, respectively. At last, the chemical shift peak at 58.95 is the saturated carbon atom attached to an oxidized sulphur atom.[45] Compared with that shown in Fig. 3A, Fig. 3B shows the chemical shift peak at 47.61, which is associated with a saturated carbon atom attached to an unoxidized sulphur atom. Interestingly the peaks of other carbon atoms in Fig. 3B show red shifts because of the oxidation of sulphur atom. In a word, we can confirm that the product of MPTS loading is oxidized and propyl-sulfonic acid group is connected to $SiO_2$ by chemical bonding successfully

**Table 1** The textural and acidic parameters of various acid catalysts.

| Entry | Catalyst | $S_{BET}$ ($m^2$/g) | $V_p$ ($cm^3$/g) | Mean $D_p$ (nm) | Total acidity (μmol/g) [a] | Acidity density (μmol/$m^2$) |
|---|---|---|---|---|---|---|
| 1 | Micro-bead silica | 350.9 | 0.84 | 11.3 | _ [c] | _ [c] |
| 2 | SA-$SiO_2$-10.6 | 345.0 | 0.68 | 11.1 | 230 | 0.66 |
| 3 | SA-$SiO_2$-22.5 | 310.3 | 0.51 | 10.5 | 340 | 1.10 |
| 4 | SA-$SiO_2$-33.1 | 273.7 | 0.43 | 9.9 | 490 | 1.79 |
| 5 | SA-$SiO_2$-40.9 | 221.1 | 0.39 | 9.6 | 610 | 2.76 |
| 6 | SA-$SiO_2$-52.0 | 160.5 | 0.33 | 8.1 | 710 | 4.42 |
| 7 | SA-$SiO_2$-60.5 | 140.9 | 0.29 | 7.3 | 840 | 5.96 |
| 8 | SA-$SiO_2$-71.9 | 109.7 | 0.17 | 6.0 | 970 | 8.84 |
| 9 | SA-$SiO_2$-83.3 | 48.3 | 0.09 | 4.9 | 1290 | 26.71 |
| 10 | $H_2SO_4$ | _ [c] | _ [c] | _ [c] | 20000 | _ [c] |
| 11 | Amberlyst-15 | 49.1 | 0.29 | 40.0 | 4530 | 92.26 |
| 12 | SBA-15-$SO_3H$ | 379.6 | 0.92 | 3.8 | 810 | 2.13 |
| 13 | Hβ (25) | 650.9 | 0.25 | 0.65 | 490 | 0.75 |
| 14 | HZSM-5 (40) | 451.7 | 0.14 | 0.54 | 320 | 0.71 |
| 15 | MCM-49 (30) | 457 | 0.46 | 0.71 | 435 | 0.95 |
| 16 | SA-$SiO_2$-60.5 [d] | 140.1 | 0.26 | 7.1 | 790 | 5.64 |
| 17 | SBA-15-$SO_3H$ [d] | 303.6 | 0.69 | 3.1 | 150 | 0.49 |

[a] Determined by $NH_3$-TPD (Fig. 3S) except SA-$SiO_2$-60.5. [b] Acidity density=total acid amount/BET surface area. [c] Undetectable. [d] After ten recycles.

The thermogravimetric analysis (TGA) of SA-$SiO_2$-60.5 catalyst is shown in Fig. 4. Firstly, a slow weight loss in the range of 0~250 ℃ was noticed. Then a sharp weight loss was observed between 250 and 400 ℃, which indicates desorption of the sulfonic groups on the surface of the micro-bead silica. The weight loss above 400 ℃ is due to the dehydration of hydroxyl groups in the pore walls of micro-bead silica.[40] Thus it can be concluded that the SA-$SiO_2$-60.5 catalyst is thermally stable and suitable for use at less than 250 ℃.

The acidity, surface area, pore volume and pore size of various acid catalysts are shown in Table 1. The sulphonic resin has the maximum acidity (4530 μmol/g) among these solid catalysts while its surface area is very poor (49.1$m^2$/g). Compared with the Amberlyst-15 resin, the SA-$SiO_2$ has larger surface area and exhibits an appropriate high acidity and pore size. Furthermore, as shown in Table 1 (Entries 1, 2, 3, 4, 5, 6, 7, 8 and 9), the acid concentration can be adjusted, and the acidity are varied from 230μmol/g to 1290μmol/g. The pore

**Table 2** Catalytic performance of various sulfo-based catalysts and zeolites in the dehydration of sorbitol.[a]

| Entry | Catalyst | Sorbitol Conv. (%) | Yield. (%) | | Others (%) [b] |
|---|---|---|---|---|---|
| | | | Isosorbide | Sorbitan | |
| 1 | SA-$SiO_2$-60.5 | 100 | 84 | 11 | 5 |
| 2 | $H_2SO_4$ | 100 | 90 | _ [c] | 7 |
| 3 | Amberlyst-15 | 93 | 71 | 5 | 24 |
| 4 | SBA-15-$SO_3H$ | 95 | 70 | _ [c] | 11 |
| 5 | Hβ (25) | 69 | 25 | 22 | 22 |
| 6 | HZSM-5 (40) | 30 | 9 | 17 | 4 |
| 7 | MCM-49 (30) | 73 | _ [c] | 29 | 14 |
| 8 | SA-$SiO_2$-60.5 [d] | 100 | 75 | 20 | 5 |
| 9 | SBA-15-$SO_3H$ [d] | 77 | 31 | 37 | 9 |

[a] Reaction condition: 120 ℃, 10 h, 1000 Pa, 50 g of sorbitol, 1.0 g of catalyst. [b] The by-products are 2,5-anhydro-d-sorbitol, 1,5-anhydro-d-sorbitol, and some others. [c] Undetectable. [d] After ten recycles.

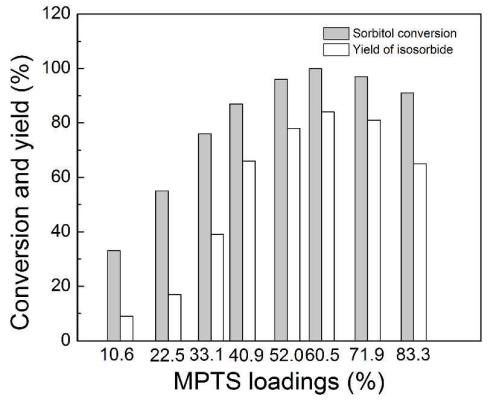


**Fig. 5** Effect of different MPTS loadings on the performance of sorbitol dehydration. Reaction condition: 50 g sorbitol, 1.0 g catalyst, 120 ℃, 10 h.

volume and pore size are decreased with the rise of MPTS content. Pore size distributions of used SA-$SiO_2$-60.5 and SBA-15-$SO_3H$ are shown in Fig. S4.

**Catalyst performance**

The catalytic performance of SA-$SiO_2$ catalysts for dehydration of sorbitol to isosorbide was evaluated in solvent free and vacuum conditions, which is helpful to remove off water from the reaction system to promote the reaction equilibrium shift to the positive direction. As shown in Scheme 1, the major dehydrated products identified are isosorbide, 1, 4-sorbitan and along with a very small amount of 3, 6-sorbitan. 2, 5-anhydro-d-sorbitol, 1, 5-anhydro-d-sorbitol and some non identified substances were all termed here as "others". To compare different catalysts, we chose various acid catalysts such as $H_2SO_4$, Amberlyst-15 resin, Hβ and HZSM-5 zeolites. The results listed in Table 2 show that Hβ(Si/Al=25) and HZSM-5(Si/Al=40) give a relatively low sorbitol conversion and yield of isosorbide. Both Amberlyst-15 resin and SBA-15-$SO_3H$ have high reactivity, but yield of isosorbide is low. Compared with those solid catalysts, the SA-$SiO_2$-60.5 catalyst exhibits the highest sorbitol conversion (100%) and yield of isosorbide (84%). This reactivity is very close to traditional homogeneous catalyst such as $H_2SO_4$.

It is worth note that although SA-$SiO_2$-60.5 doesn't offer the maximum acidity, but displays good reaction performance (see Table 2). Compared other reported hydrophilic catalysts in Table S2, SA-$SiO_2$-60.5 provides a higher yield of isosorbide and the reaction condition is moderate. This should be attributed to its suitable large pore size and high surface area (see Tab 1). Thus it is beneficial to mass transfer process, thereby inhibiting coke forming.

Fig. 5 shows the activity of dehydration of sorbitol over various SA-$SiO_2$-X at 120 ℃ for 10 h. With increasing the MPTS loading from 10.6% to 40.9%, the yield of isosorbide increases obviously. When the MPTS loading increases from

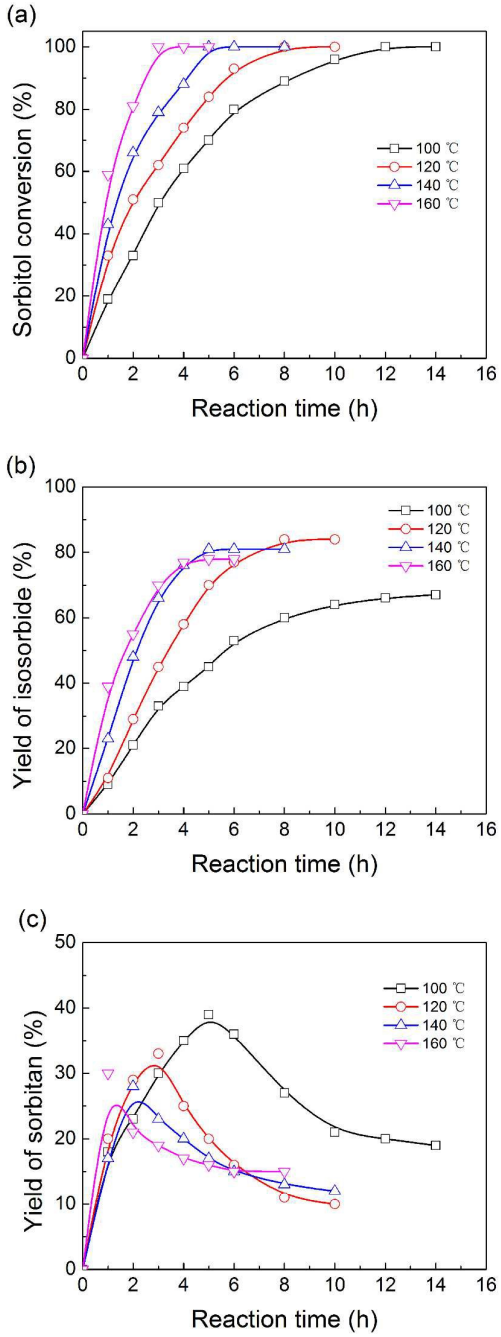


**Fig. 6** Effect of reaction temperature on the performance of sorbitol dehydration. Reaction condition: 10 g sorbitol, 0.2 g catalyst, sorbitol conversion (a), yield of isosorbide (b), yield of sorbitan (c).

40.9% to 60.5%, the growth rate of isosorbide yield slows down. Thereafter, with the continued increase of MPTS loading, the yield of isosorbide is decreased. Yield of isosorbide and conversion of sorbitol are maximised at 60.5% MPTS loading.

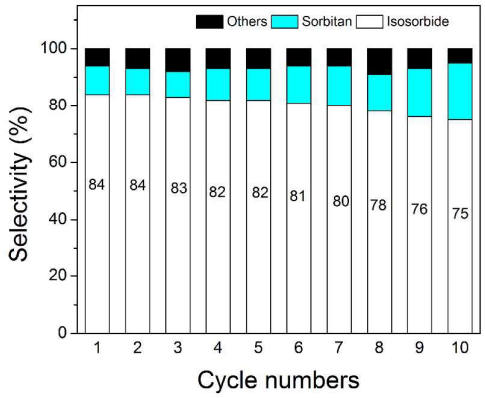


**Fig. 7** Reuse of SA-$SiO_2$-60.5 in the dehydration of sorbitol at 120 ℃ for 10 h under vacuum.

This phenomenon suggests that the further increase of MPTS loading (above 60.5%) will block the pore of micro-bead silica in physics.[40] Thus it seriously obstructs the internal diffusion and transfer of reactants and decreases the yield of isosorbide.

The influence of reaction temperature on the dehydration reaction was investigated, and the results are shown in Fig. 6. As shown in Fig. 6a, the conversion of sorbitol is 100% at 100~160 ℃. At 100 ℃, the yield of isosorbide is low, ca. 60%. With increasing the dehydration reaction temperature to 120 ℃, the yield of isosorbide reaches the highest value (84%), and then decreases with further increasing the temperature to 160℃ (see Fig. 6b), since more coke during the test is formed. But the sorbitan yield, a main intermediate product,[29, 46] decreases as the temperature increasing (see Fig. 6c). These demonstrated that an appropriate reaction temperature was crucial for achieving a high yield of isosorbide.[47] The highest catalytic performance is observed at 120 ℃ for 10 h under vacuum with 2% SA-$SiO_2$-60.5 (100% conversion of sorbitol and 84% yield of isosorbide).

The recyclability is of great importance for applying a solid catalyst in industrial production. After reaction, the SA-$SiO_2$-60.5 has been washed in ultrasonic pool with water and glycol dimethyl ether to evaluate its recyclability, and the results are shown in Fig. 7. After being reused for 10 times, sorbitol conversion is still 100% and the yield of isosorbide decreases only slightly. Compared with other zeolites,[48] the regeneration process does not require calcination and the synthesis does not need surfactant or template so that the cost can be reduced. All the results indicate that the SA-$SiO_2$-60.5 exhibits excellent stability and low-cost.

As shown in Table S2, most of the hydrophilic catalysts such as oxides, phosphates and sulfated materials showed a relatively high reactivity compared with other hydrophobic catalysts, which makes us believe that the high reactivity and stability of SA-$SiO_2$-60.5 is derived from its high surface hydrophilicity. As observed in Fig. 8, the sorbitol and isosorbide contact angle on SA-$SiO_2$-60.5 is about 12.1° and

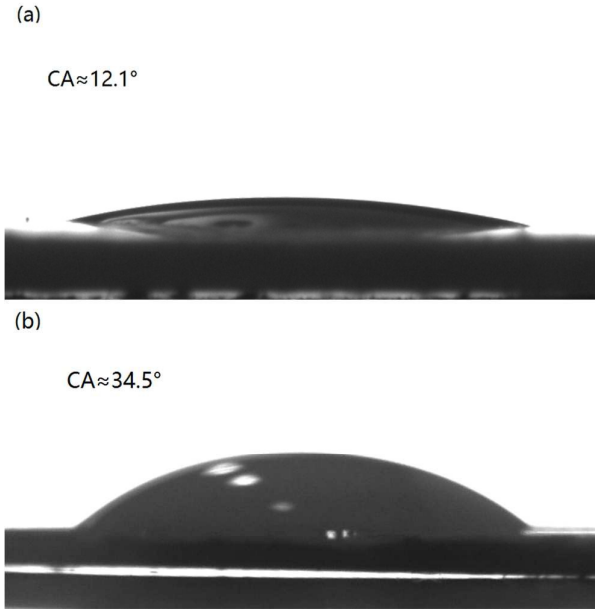


**Fig. 8** Sorbitol droplet contact angle (CA) on SA-$SiO_2$-60.5 (a) and isosorbide droplet contact angle on SA-$SiO_2$-60.5 (b).

34.5°, respectively. This indicates that SA-$SiO_2$-60.5 has a high hydrophilic surface, and its surface affinity to sorbitol is stronger than that to isosorbide. Scheme 3 shows the process of sorbitol dehydration to isosorbide. The high surface hydrophilicity and different surface affinity of SA-$SiO_2$-60.5 catalyst is in favor of the feed (sorbitol) reaching and the product (isosorbide) leaving active site rapidly, thus suppresses the sequential reactions which cause coke formation. Under the reaction conditions (100~160 ℃, 650~1000 Pa), water, formed in the reaction, can be removed out of the reactor instantly, although it is a more polar molecule than sorbitol and isosorbide. This avoids the competitive adsorption of water on the surface of the catalyst with high hydrophilicity. As a regeneration treatment in each cycle, the catalyst was washed with water and glycol dimethyl ether. Moreover, the high surface hydrophilicity of SA-$SiO_2$-60.5 catalyst makes the depositing coke, which is hydrophobic, washed away easily. So the catalyst activity is restored. Therefore, the physical and chemical properties of SA-$SiO_2$-60.5 are also stable. For example, after recycle for ten times, the SA-$SiO_2$-60.5 still gave acid site at 790 μmol/g, which slightly lower than that of the fresh catalyst (840 μmol/g). On the contrary, the acid site of SBA-15-$SO_3H$ almost decreased to none, and its recyclability was very poor. From the TGA (Fig. S1) and FT-IR curves (Fig. 1b), the curves of SA-$SiO_2$-60.5 remain almost unchanged after ten recycles respectively. It can be concluded that the SA-$SiO_2$-60.5 is easily regenerated and exhibits good stability.

## Conclusions

We have found that SA-$SiO_2$-60.5 is a highly effective solid acid catalyst for dehydration of sorbitol into isosorbide in solvent-free condition. The used catalyst can be easily regenerated by washing with water and glycol dimethyl ether. And the catalyst displays good stability because it can be reused for 10 times without significant loss of activity and selectivity. The excellent performance of the SA-$SiO_2$-60.5 is attributed to its suitable large pore diameter and high surface hydrophilicity that is beneficial to the feed adsorption and the product desorption, and inhibits the deposition of coke. Thus, the catalyst—SA-$SiO_2$ prepared in this work, has high potential for conversion of the most abundant biomass into the platform chemicals.

## Acknowledgements

This work was supported by Jiangsu province science & technology innovation project (BY2014037-12), and the Project Funded by the Priority Academic Program Development of Jiangsu Higher Education Institutions.

## References

1. K. Saravanan, B. Tyagi, R. S. Shukla and H. C. Bajaj, *Applied Catalysis B: Environmental*, 2015, **172–173**, 108-115.
2. L. Wang, D. Li, H. Watanabe, M. Tamura, Y. Nakagawa and K. Tomishige, *Applied Catalysis B: Environmental*, 2014, **150–151**, 82-92.
3. N. Li, G. A. Tompsett, T. Zhang, J. Shi, C. E. Wyman and G. W. Huber, *Green Chemistry*, 2011, **13**, 91-101.
4. Y. Yang, C.-w. Hu and M. M. Abu-Omar, *Green Chemistry*, 2012, **14**, 509-513.
5. Y. Liu, L. Chen, T. Wang, Y. Xu, Q. Zhang, L. Ma, Y. Liao and N. Shi, *RSC Advances*, 2014, **4**, 52402-52409.
6. P. Gallezot, *Topics in Catalysis*, 2010, **53**, 1209-1213.
7. T. Deng, X. Cui, Y. Qi, Y. Wang, X. Hou and Y. Zhu, *Chemical Communications*, 2012, **48**, 5494-5496.
8. C.-H. Zhou, X. Xia, C.-X. Lin, D.-S. Tong and J. Beltramini, *Chemical Society Reviews*, 2011, **40**, 5588-5617.
9. B. Zhang, Y. Zhu, G. Ding, H. Zheng and Y. Li, *Green Chemistry*, 2012, **14**, 3402-3409.
10. H. Kobayashi, H. Matsuhashi, T. Komanoya, K. Hara and A. Fukuoka, *Chemical Communications*, 2011, **47**, 2366-2368.
11. M. Liu, W. Deng, Q. Zhang, Y. Wang and Y. Wang, *Chemical Communications*, 2011, **47**, 9717-9719.
12. Y. Morita, S. Furusato, A. Takagaki, S. Hayashi, R. Kikuchi and S. T. Oyama, *ChemSusChem*, 2014, **7**, 748-752.
13. S. Van de Vyver, J. Geboers, M. Dusselier, H. Schepers, T. Vosch, L. Zhang, G. Van Tendeloo, P. A. Jacobs and B. F. Sels, *ChemSusChem*, 2010, **3**, 698-701.
14. J. J. Bozell and G. R. Petersen, *Green Chemistry*, 2010, **12**, 539-554.
15. H. Kobayashi and A. Fukuoka, *Green Chemistry*, 2013, **15**, 1740-1763.
16. H.-J. L. Gwi-Taek Jeong, Hae-Sung Kim, Don-Hee Park, *Applied Biochemistry and Biotechnology*, 2006, **129**, 265–277.
17. J. Xia, D. Yu, Y. Hu, B. Zou, P. Sun, H. Li and H. Huang, *Catalysis Communications*, 2011, **12**, 544-547.
18. M. Rose and R. Palkovits, *ChemSusChem*, 2012, **5**, 167-176.
19. P. Sun, X. Long, H. He, C. Xia and F. Li, *ChemSusChem*, 2013, **6**, 2190-2197.
20. A. Yamaguchi, N. Hiyoshi, O. Sato and M. Shirai, *Green Chemistry*, 2011, **13**, 873-881.
21. G. Flèche and M. Huchette, *Starch - Stärke*, 1986, **38**, 26-30.
22. A. Yamaguchi, O. Sato, N. Mimura and M. Shirai, *RSC Advances*, 2014, **4**, 45575-45578.
23. A. Kamimura, K. Murata, Y. Tanaka, T. Okagawa, H. Matsumoto, K. Kaiso and M. Yoshimoto, *ChemSusChem*, 2014, **7**, 3257-3259.
24. N. A. Khan, D. K. Mishra, I. Ahmed, J. W. Yoon, J.-S. Hwang and S. H. Jhung, *Applied Catalysis A: General*, 2013, **452**, 34-38.
25. A. A. Dabbawala, D. K. Mishra and J.-S. Hwang, *Catalysis Communications*, 2013, **42**, 1-5.
26. X. Zhang, D. Yu, J. Zhao, W. Zhang, Y. Dong and H. Huang, *Catalysis Communications*, 2014, **43**, 29-33.
27. J. Li, A. Spina, J. A. Moulijn and M. Makkee, *Catalysis Science & Technology*, 2013, **3**, 1540-1546.
28. O. A. Rusu, W. F. Hoelderich, H. Wyart and M. Ibert, *Applied Catalysis B: Environmental*, 2015, **176–177**, 139-149.
29. R. M. de Almeida , J. Li, C. Nederlof, P. O'Connor, M. Makkee and J. A. Moulijn, *ChemSusChem*, 2010, **3**, 325-328.
30. J. Li, W. Buijs, R. J. Berger, J. A. Moulijn and M. Makkee, *Catalysis Science & Technology*, 2014, **4**, 152-163.
31. N. A. Khan, D. K. Mishra, J.-S. Hwang, Y.-W. Kwak and S. H. Jhung, *Research on Chemical Intermediates*, 2011, **37**, 1231-1238.
32. Y. Xiu, A. Chen, X. Liu, C. Chen, J. Chen, L. Guo, R. Zhang and Z. Hou, *RSC Advances*, 2015, **5**, 28233-28241.
33. J. Zhang, L. Wang, F. Liu, X. Meng, J. Mao and F.-S. Xiao, *Catalysis Today*, 2015, **242, Part B**, 249-254.
34. M. A. Z. P. Salehi, F. Shirinic and M. Baghbanzadeh, *Current Organic Chemistry*, 2006, **10**, 2171-2189.
35. Z. Hasan and S. H. Jhung, *European Journal of Inorganic Chemistry*, 2014, **2014**, 3420-3426.
36. A. A. Dabbawala, J. J. Park, A. H. Valekar, D. K. Mishra and J.-S. Hwang, *Catalysis Communications*, 2015, **69**, 207-211.
37. W. N. P. van der Graaff, K. G. Olvera, E. A. Pidko and E. J. M. Hensen, *Journal of Molecular Catalysis A: Chemical*, 2014, **388–389**, 81-89.
38. M. H. Valkenberg, C. deCastro and W. F. Holderich, *Green Chemistry*, 2002, **4**, 88-93.
39. Z. W. Y. Huang, Y. Liu and Q. Ren, *Journal of Chemical Engineering of Chinese Universities*, 2008, **22**, 721-724.
40. J. D. Y. Zhang, Y. Shan, Y. Zhou, G. Wang and M. Li, *Journal of Chemical Engineering of Chinese Universities*, 2010, **24**, 825-829.
41. W. Zhou, J. Liu, J. Pan, F. a. Sun, M. He and Q. Chen, *Catalysis Communications*, 2015, **69**, 1-4.
42. B. Xue, J. Xu, C. Xu, R. Wu, Y. Li and K. Zhang, *Catalysis Communications*, 2010, **12**, 95-99.
43. Y. Guo, K. Li, X. Yu and J. H. Clark, *Applied Catalysis B: Environmental*, 2008, **81**, 182-191.
44. S. Hamoudi and S. Kaliaguine, *Microporous and Mesoporous Materials*, 2003, **59**, 195-204.

45. C. Pirez, A. F. Lee, J. C. Manayil, C. M. A. Parlett and K. Wilson, *Green Chemistry*, 2014, **16**, 4506-4509.
46. N. Li and G. W. Huber, *Journal of Catalysis*, 2010, **270**, 48-59.
47. R. Otomo, T. Yokoi and T. Tatsumi, *Applied Catalysis A: General*, 2015, **505**, 28-35.
48. H. Kobayashi, H. Yokoyama, B. Feng and A. Fukuoka, *Green Chemistry*, 2015, **17**, 2732-2735.

## *Graphical Abstract*

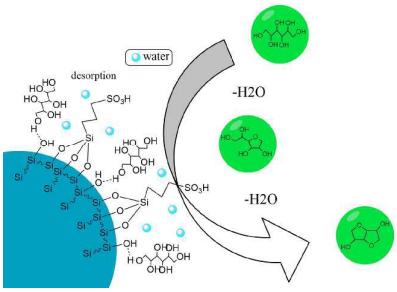


Large pore diameter and hydrophilic surface of SA-$SiO_2$-60.5 is beneficial to sorbitol adsorption and isosorbide desorption, and inhibits deposition of coke.